Geotechnical and Geophysical Site Characterisation 5 – Lehane, Acosta-Martínez & Kelly (Eds)

Virtual T-bar penetrometer tests using Discrete Element Method

L.S. Carvalho, J.R.M.S. Oliveira, C.A.B. Vasconcellos & M.E.S Marques
Military Institute of Engineering, Rio de Janeiro, Brazil

M.G. Teixeira
Federal University of Rio de Janeiro, Rio de Janeiro, Brazil

J.A. Lukiantchuki
State University of Maringá, Maringá, Paraná

ABSTRACT: The Discrete Element Method (DEM) is an important tool to investigate soil-structure interaction problems involving dynamics and large strains. This technique can be applied to reproduce the behaviour of granular soils but can also be used to simulate the behaviour of very soft clay, where the material performs as a viscous fluid. Unlike the Finite Element Method (FEM), in the DEM the elements are discontinuous, allowing large strain simulations with no need for remeshing, which is a complex and time spending technique. In that way, a DEM software so-called VISED, was developed based on principles of equilibrium and interaction between the elements. The program algorithm is an adapted version of the software Munjiza-NBS and uses the following chain of processes: calculation of velocities and positions, contacts checking, calculation of contact forces and calculation of external forces and links. VISED takes into account two forces of contact between the elements: normal and tangential. The normal force uses as parameters: stiffness, damping, interpenetration between particles and velocity. On the other hand, the tangential force uses as parameters: stiffness, damping, velocity and dynamic friction. The links are calculated using an elastic perfectly plastic model, where an elasticity modulus, a yield stress and a limit strain are needed. The aim of this paper is to present a series of T-bar penetrometer virtual tests in order to evaluate the performance of the program. Thus, input parameters such as dynamic friction and damping were changed in a specific range to evaluate the influence of this variation in the final results. The final T-bar penetration test in the soil was compared with data from real tests in clays.

1 INTRODUCTION

The numerical modelling of soil behaviour is a very important tool to solve engineering problems, although quite challenging regarding some types of soils and loading conditions. That is the case of dry non-cohesive soils, where the material is clearly discontinuous and constituted of independent particles. Another example is the case of very soft clays, where regular loadings are associated with large deformations.

The Finite Element Method (FEM) is by far the most frequent numerical method applied for soil simulation in academy and industry. However, there are some restrictions associated with the simulation of problems involving discontinuous materials and large deformations.

In that way, the Discrete Element Method (DEM) shows up as a very promising tool due to some particular characteristics. The method is based on a number of non-deformable elements that constitute the material and these elements interact with each other through predefined bond conditions. When a limit condition is reached, the bond is broken and the elements are disconnected.

Thus, regarding situations where large deformations are expected, the numerical simulation is feasible with no need of any remeshing technique or equivalent procedure, once the elements are naturally rearranged in a new configuration.

The aim of this paper is to present a series of T-bar penetrometer virtual tests in order to evaluate the performance of the program. Thus, input parameters such as dynamic friction and damping were changed in a specific range to evaluate the influence of this variation in the final results. The final T-bar penetration test in the soil was compared with data from real tests in clays.

2 THE T-BAR PENETRATION TEST

The T-Bar penetration test was first developed as a mini tool to assess the undrained shear strength in

reduced models in geotechnical centrifuge tests (Stewart & Randolph 1991). After a considerable number of modellings, a real size tool was developed and used in field tests (Stewart & Randolph 1994).

Academic applications of the T-bar penetrometer in Brazil were conducted by Macedo (2004) in a series of field tests in the very soft grey clay of Rio de Janeiro. The results were compared with piezocone and vane tests carried out at the same place, as well as triaxial tests with samples taken from the same site with very good agreement.

Jannuzi (2009) also conducted T-bar field tests in Sarapuí II site in Rio de Janeiro, which is a very well known deposit, also with very good agreement. The author concluded that the T-bar test is an important tool to assess the undrained shear strength continuous profile of very soft clay layers.

As far as the Brazilian centrifuge modeling scenario is concerned, Oliveira & Almeida (2010) conducted a series of centrifuge tests to evaluate the pore-pressure generation around the bar in cyclic T-bar tests on clayey soil. Oliveira et al. (2010) also investigated the influence of the T-bar penetration rate on the penetrometer resistance. Finally, Almeida et al. (2013) studied the variation of the bearing capacity factor of T-bar penetration tests at shallow depths in clayey soils.

The T-Bar tool itself is a 50 mm diameter and 200 mm length bar which is attached to an adapted piezocone rod as presented in Figure 1. The bar is pushed against the soil at a 2 cm/s rate and the soil resistance is measured through a load cell positioned at the rod just above the bar.

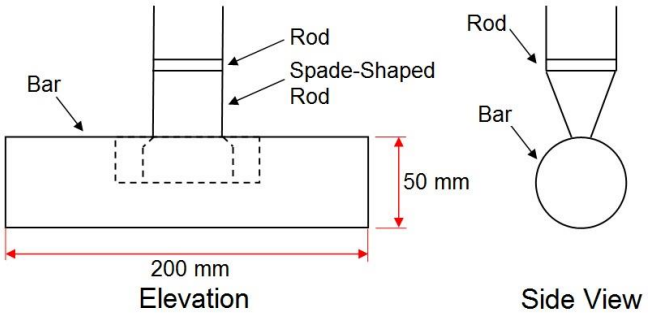

Figure 1. Field T-bar penetrometer (adapted from Stewart & Randolph 1994).

The undrained shear strength (S_u) is calculated using the limiting pressure on a circular surface in cohesive soil as proposed by Randolph & Houlsby (1984) in Equation (1), where P is the limit force acting on the bar, D is the bar diameter and N_b is the loading factor.

$$P = S_u \cdot D \cdot N_b \quad (1)$$

3 THE GEOTECHNICAL MODEL

The natural water content Brazilian coastal very soft clays are sometimes higher than its liquid limit, thus these soils behave as a fluid when remolded. When in fluid state the behavior of the Clay is mainly due to electrochemical forces between clay particles, water and ions that compose the soil. Mitchell (2005) proposes that the determination of these forces is very complex due to soil composition and the high variation of environmental factors that act during soil formation. However, Mitchell (2005) presented a qualitative analysis of the attraction and repulsive forces showing that when the particles interact, there is an attraction force increasing to a maximum value and then decreasing until changing to repulsive force, as seen in Figure 2.

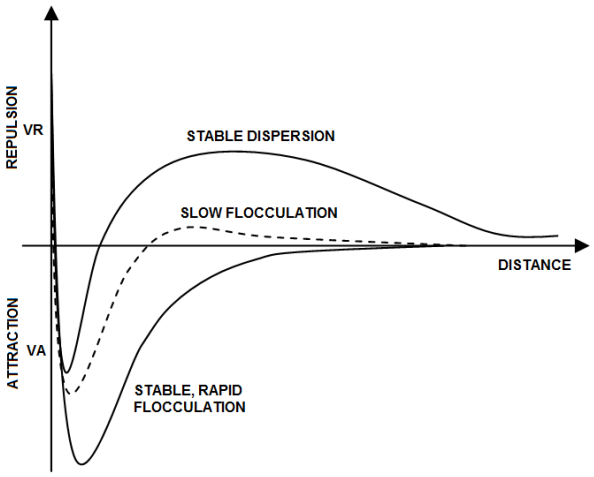

Figure 2. Interaction electrochemical forces between clay particles (after Mitchell, 2005).

From the numerical model point of view, it is not possible to consider the individual clay particles due to time processing. Therefore, an arrangement, where each discrete element is considered as a soil agglomerate composed by clay particles, water and ions, is proposed for the numerical model. The physical characteristics of the soil, as liquidity and cohesiveness are represented in the numerical model as field forces which will be discussed later.

4 THE VISED PROGRAM

4.1 *Introduction*

The Discrete Element Method visualization software – VISED 3.7, developed in C++ by Minato et al. (2009), uses the graphic library OpenGL© capable of generating graphics in real time with many effects such as texture and animation. The OpenGL Utility Tools (GLUT) is used to create special input and output features.

The software was initially developed to simulate materials that behave as discontinuous matter such

as non-cohesive soils, but is also being used to emulate very soft soils in large strain conditions.

The numerical method adopted for the VISED 3.7 software is the discrete element method, which deals with each element as a rigid and independent particle. The elements interact with each other through predefined bond conditions.

Silva et al. (2011) presents a DEM simulation of the fall cone test using the VISED 3.7 software with good agreement.

4.2 *The Algorithm Procedure*

The software uses the interaction between particles and equilibrium principles to calculate the numerical solution. The developed algorithm combines four main processes: collision detection between particles; analysis of interaction forces between particles; fixations and external forces calculation; and new velocities and position calculation.

The collision detection between particles uses the Munjiza-NBS (No Binary Search) algorithm, described on Munjiza (2004), which employs direct mapping to detect contact between elements and thus compute the collision forces.

The interaction forces between particles can be divided in two components: contact forces and field forces. In this work, the field forces are modelled based on the Morse potential and will be discussed later.

The contact forces between particles have a normal and a tangential component. The normal component (F_n) uses as parameters the normal stiffness (k_n) associated with the elements interpenetration (u_n), and the normal dumping (c_n) associated with the normal component of the relative velocity between elements (v_n) as shown in Equation (2).

$$F_n = k_n \cdot u_n + c_n \cdot v_n \tag{2}$$

The tangential component (F_t) uses as parameters the minimum value of the force, calculated based on the tangential stiffness (k_t), and the force calculated based on the dynamic friction (μ), as shown in Equation (3). The tangential stiffness is associated with the tangential damping (c_t) and the tangential component of the relative velocity (v_t), while the dynamic friction is associated with the normal force (F_n),

$$F_t = \min\left\lfloor k_t \int v_t \cdot dt + v_t \cdot c_t ; F_n \cdot \mu \right\rfloor \tag{3}$$

The bond forces are generated by the deformations between the virtual bond elements which have an elasto-plastic behaviour. Therefore, the forces are calculated using the following parameters: the Young modulus (E), yield stress (σ_E) and the strain at rupture (ε_r). These parameters are input data for the program. In the case of the simulations presented in this work, the bond elements are not used and therefore not considered in the calculations.

The velocities and position calculations of each element are processed as solutions of the differential equilibrium equations $F = md^2u/dt^2$, based on the initial pre-established conditions. The algorithm uses the Central Differences Method (Krysyl & Belytschko 1998) to solve the equations numerically.

4.3 *Field Forces*

The program allows the implementation of many different ways of interaction forces between the elements, with intensity, direction and signal determined by the programmer.

This work adopted forces with intermolecular interaction characteristics, considering an attraction between the elements for distances greater than a minimum value and repulsion for distances smaller than the same minimum value. This behaviour is very similar to the one described by Mitchell (2005) and presented in Section 3.

The formulation of this interaction is based on the interaction force due to Morse potential which is an interatomic interaction model. The intensity of the force is obtained taking the derivative of the potential with respect to the distance between the elements. Equation (4) and Equation (5) show, respectively, the Morse potential and the interaction force between the elements, where: d is the depth of the potential and represents the dissociation energy (necessary energy to break the link between the elements); k is related with the width of the potential and has the dimension of m^{-1}; x is the distance between the centers of the elements; and $dist$ is the equilibrium distance, i.e., the distance between the elements where the force is zero.

$$E_p(x) = -d + d\left(1 - e^{-k(x-dist)}\right)^2 \tag{4}$$

$$E_p(x) = \frac{-dE_p(x)}{dx} = -2dk\left(1 - e^{-k(x-dist)}\right)e^{-k(x-dist)} \tag{5}$$

The force F_p acts in the direction of the vector that links the centers of the elements and might be positive, when the elements are being attracted, or negative, when they are being repulsed.

Figure 3 shows the intensity of the field force as a function of the distance between the elements. In this work, this force aims to emulate the interaction between the clay particles. The behaviour shown in Figure 3 is similar to the one shown in Figure 2. In that way, the field forces role the play of the clay particles electrochemical interaction forces as the main link between the clay particles.

The output of the VISED program is the frames sequence of the simulation and a text file, both saved in a rate predefined by the user. With the DAT file the program can shows an animation of the simulation.

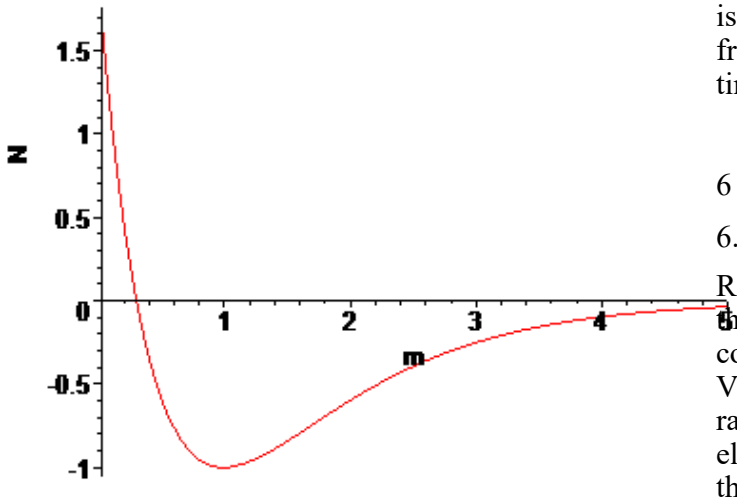

Figure 3. Field force with *dist* = 0.3, k = 1, d = 2 and x = 5.

5 SOFT SOIL CHARACTERISTICS

Brazilian coastal soft soils are very compressible, organic and with very low S_u values. The soil used for comparison with the simulations in this work is a very soft clay from Guanabara Bay, Rio de Janeiro State. Table 1 shows the soft clay parameters from several field and laboratory tests.

Table 1. Soft soil parameters.

Soil Parameter	Values
Plasticity Index (PI)	90% – 120%
Liquid Limit (w_L)	140% – 180%
Plastic Limit (w_P)	50%
Void Ratio (e)	3.6 – 4.5
Density of Grains (G_S)	2.49 – 2.68 kN/m^3
Specific Submerged Weight (γ')	2.5 – 4.5 kN/m^3
Coefficient of Consolidation (c_v)	3x10^{-8} – 5x10^{-9} m^2/s

Figure 4 shows the average S_u prototype profile for this clay from T-bar centrifuge tests carried out by Oliveira et al. (2010).

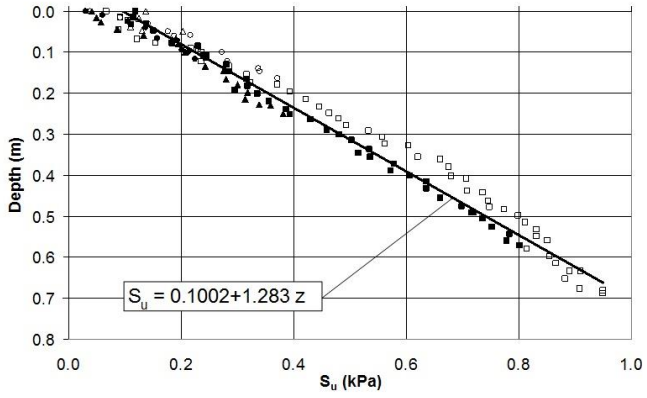

Figure 4. Prototype undrained shear strength profile from centrifuge tests (after Oliveira et al. 2010).

These soft soils are very heterogeneous and there is a scatter of the Young Modulus values obtained from several triaxial tests, thus the E values were estimated as $E = 300S_u$ (Oliveira et al., 2010).

6 DEM SIMULATION OF T-BAR TEST

6.1 *Model Dimensions*

Regarding the determination of the dimensions of the virtual model, it was necessary to take into account the time to achieve convergence when running VISED. This time of processing is function of the radius of the discrete elements as well as how many elements were used to represent the soil domain. In this particular case of study, a scale factor of N = 0.25 was found to be more appropriate once it would reduce processing time.

Thus, for a 4.4 m high by 1.0 m width soil domain, 5,920 discrete elements were used with a 10 mm radius each. The T-Bar (prototype diameter of 50 mm) was modeled as a sole discrete element with a 100 mm radius. All modeling relationships were considered when calculating results back from model to prototype scale.

6.2 *Contact Forces Input Parameters*

Table 2 presents the parameters VISED used to obtain the contact forces. The damping ($c_{n,t}$) value was adopted as proposed by Silva et al. (2011) and the Young modulus (E) was considered as function of the S_u value at 0.5m.

Table 2. Contact forces input parameters.

Parameter	Values
Submerged Specific Weight (γ')	3.5 kN/m^3
Young Modulus (E)	222 kPa
Yield Stress (σ_R)	4.94 kPa
Deformation at Rupture (ε_R)	0.022
Friction (μ)	0.05
Specific Submerged Weight (γ')	2.5 – 4.5 kN/m^3
Damping ($c_{n,t}$)	3.5 kg/s

6.3 *Field Forces Input Parameters*

The parameter *dist* was considered constant and equal to 4x10^{-2} m. This value, kept the elements, when subjected to a contact force, under space equilibrium, thus decreasing the number of elements necessary to occupy the same area of domain and decreasing processing time.

It was also considered for the computation of field forces a dumping parameter, proportional to the component of relative velocity between elements at the direction of the vector that connects the centers of these elements. This parameter (h), which is associated to relative velocity, is also called damping and has the same physical meaning as the damping used for computation of the contact forces.

Three different series of simulations were carried out varying d, k and h as shown in Table 3. The 36

tests were conducted with 5,920 discrete elements, and a single element representing the T-bar. The simulation time was 60 s and processing time was average 15h for the following computer configuration: Intel® Core ™ Quad CPU Q9550 @ 2.83 GHz, 3.24 GB RAM.

Table 3. Field force parameters.

Range = 0.1m $k = 60$ m^{-1} $h = 500$ kg/s *Dist* = 4 x 10^{-2} m		*Range = 0.1m* $d = 5.2$ x 10^{-2} J $h = 500$ kg/s *Dist* = 4 x 10^{-2} m		*Range = 0.1m* $d = 5.2$ x 10^{-2} J $k = 60$ m^{-1} *Dist* = 4 x 10^{-2} m	
Model	d (J)	Model	k (m^{-1})	Model	h (kg/s)
1.1	5.2 x 10^{-2}	2.1	30	3.1	1
1.2	5.4 x 10^{-2}	2.2	35	3.2	10
1.3	5.6 x 10^{-2}	2.3	65	3.3	50
1.4	5.8 x 10^{-2}	2.4	70	3.4	100
1.5	6.0 x 10^{-2}	-	-	3.5	550
1.6	6.2 x 10^{-2}	-	-	3.6	600
1.7	6.4 x 10^{-2}	-	-	3.7	650
1.8	6.6 x 10^{-2}	-	-	3.8	700
1.9	7.0 x 10^{-2}	-	-	3.9	750
1.10	7.5 x 10^{-2}	-	-	3.10	1000
1.11	8.0 x 10^{-2}	-	-	3.11	1250
1.12	8.5 x 10^{-2}	-	-	3.12	1500
1.13	9.0 x 10^{-2}	-	-	3.13	1750
1.14	9.7 x 10^{-2}	-	-	3.14	2000
1.15	10.5 x 10^{-2}	-	-	-	-
1.16	11.5 x 10^{-2}	-	-	-	-
1.17	30.0 x 10^{-2}	-	-	-	-
1.18	40.0 x 10^{-2}	-	-	-	-

7 RESULTS AND DISCUSSION

Figure 5 shows the discrete elements set for the T-bar depth ratios H/D = 50%, 75%, 100% and 125%. It was observed that the elements flowed around the bar as expected for a very soft clay soil.

For each virtual test a S_u profile was obtained and the tendency line for the computed data was compared with the expected profile line from Figure 4. Virtual tests and real tests were then compared by analyzing the angular coefficient (a) and the linear coefficient (b) of these profiles ($S_u = a.z + b$). Table 4 presents the angular and linear coefficients of the virtual tests for each model presented in Table 3.

Series 1 results show that the variation of the parameter d did not affect significantly the inclination of the S_u profile, i.e., the angular coefficient of the tendency line. However, model 1.18 was an exception with values much lower than the other ones. It was also observed that the increase of d parameter increased the dispersion of the S_u values, increasing the line R^2.

Regarding Series 2, the k values adopted for the tests 2.1 and 2.2 conducted to repulsion values lower than expected, causing superposition of the elements at the bottom of the domain.

Series 3 show that the increase in h caused an increase of the inclination of the S_u profile, as well as the R^2 of the tendency line, i.e., the dispersion of the data.

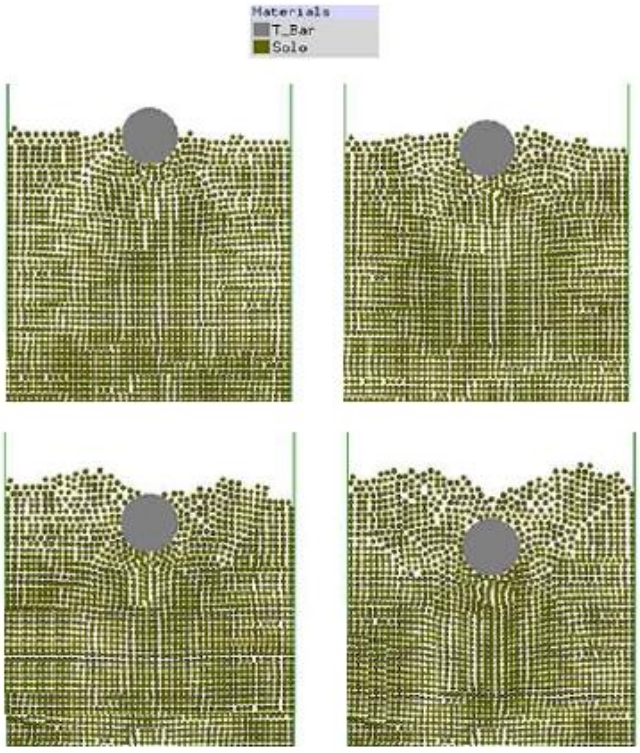

Figure 5. Visualization of a T-bar virtual test with depth ratios H/D = 50%, 75%, 100% and 125%.

Table 4. Results of the angular and linear coefficients for the virtual T-bar tests profiles.

Range = 0.1m $k = 60$ m^{-1} $h = 500$ kg/s *Dist* = 4 x 10^{-2} m			*Range = 0.1m* $d = 5.2$ x 10^{-2} J $h = 500$ kg/s *Dist* = 4 x 10^{-2} m			*Range = 0.1m* $d = 5.2$ x 10^{-2} J $k = 60$ m^{-1} *Dist* = 4 x 10^{-2} m		
Model	a	b	Model	a	b	Model	a	b
1.1	-0.71	0.12	3.1	-0.08	0.44	3.1	0.00	-0.11
1.2	-0.68	0.10	2.2	-3.44	-0.29	3.2	0.02	0.07
1.3	-0.75	0.14	2.3	-0.66	0.12	3.3	-0.02	0.09
1.4	-0.67	0.14	2.4	-0.66	0.09	3.4	-0.24	0.09
1.5	-0.64	0.14	-	-	-	3.5	-0.72	0.11
1.6	-0.71	0.08	-	-	-	3.6	-0.77	0.13
1.7	-0.73	0.14	-	-	-	3.7	-0.81	0.13
1.8	-0.76	0.10	-	-	-	3.8	-0.88	0.12
1.9	-0.69	0.14	-	-	-	3.9	-0.94	0.10
1.10	-0.66	0.12	-	-	-	3.10	-1.07	0.13
1.11	-0.64	0.13	-	-	-	3.11	-1.23	0.14
1.12	-0.64	0.11	-	-	-	3.12	-1.32	0.20
1.13	-0.70	0.13	-	-	-	3.13	-1.51	0.17
1.14	-0.64	0.14	-	-	-	3.14	-1.45	0.26
1.15	-0.64	0.11	-	-	-	-	-	-
1.16	-0.76	0.14	-	-	-	-	-	-
1.17	-0.70	0.15	-	-	-	-	-	-
1.18	-0.37	0.15	-	-	-	-	-	-

Figure 6 shows the output of the virtual test 3.11, which was the best result, along with its tendency line and the real test line, as shown in Figure 4. The tendency lines are almost coincident, although dispersion seems to be greater in the virtual data than in the real data.

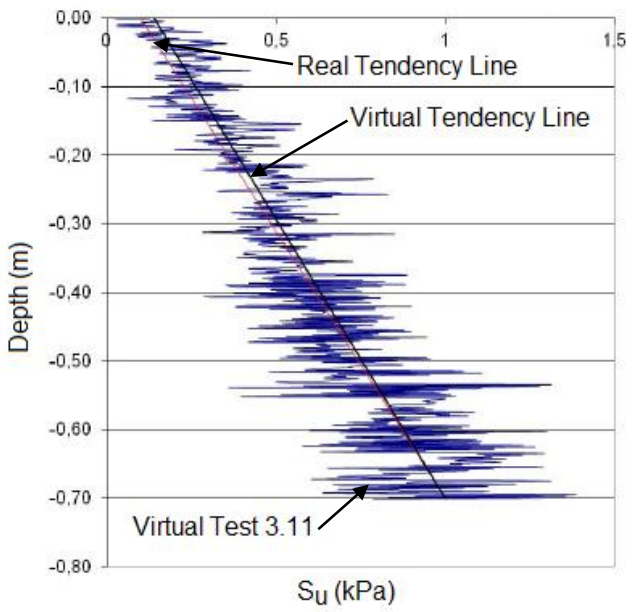

Figure 6. Result of the virtual test 3.11 along with its tendency line and the real test tendency line.

Graphic output files from VISED allow observation of the behaviour of the elements during the test. Figure 7 shows the formation of a triangle below the bar which stays in the same relative position while the other elements seem to flow around the pipe, as expected.

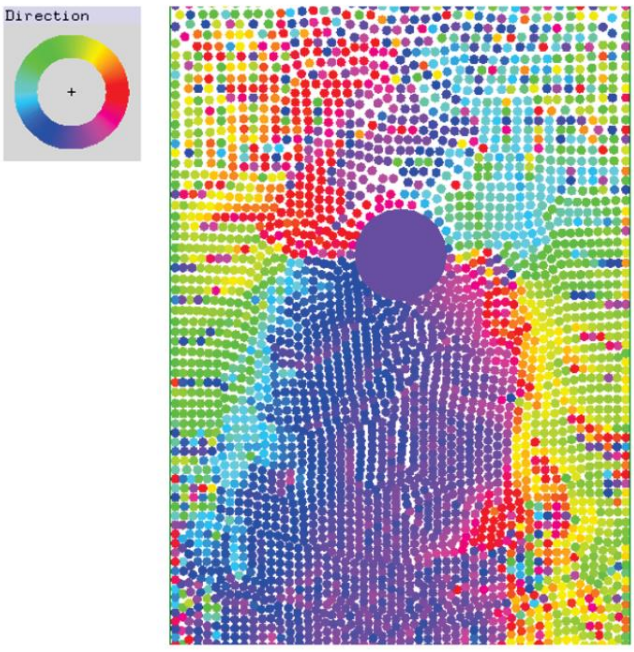

Figure 7. Visualization of the directions of the elements during a T-bar virtual test.

8 CONCLUSIONS

The use of field forces was fundamental to give the model soil cohesion characteristics which allowed virtual tests closer to real results. Although some data dispersion was expected, the virtual values show to be fairly more dispersive than the real ones. The parameters used in the analysis stays as the major problem once they are not classical geotechnical parameters and can be hard to evaluate.

The DEM method dealt with the large deformations problem without any difficulties and show to be a promising tool for geotechnical simulation of very soft soils, although further investigations are needed.

9 REFERENCES

Almeida, M.S.S., Oliveira, J.R.M.S., Rammah, K.I. & Trejo, P.C. 2013. Investigation of bearing capacity factor of T-bar penetrometer. Journal of Geo-Engineering Sciences 1, No. 1, 1–12, DOI 10.3233/JGS-13005.

Jannuzi, G.M.F. 2009. Characterization of the Sarapuí II soft soil deposit through field tests (in Portuguese). Federal University of Rio de Janeiro: M.Sc. Thesis.

Krysyl, P. & Belytschko, T. 1998. Object-Oriented Parallelization of Explicit Structural Dynamics with PVM. Pennsylvania: Computers & Structures, v. 66.

Macedo, E.O. 2004. Investigations of the in-situ undrained shear strength through cylinder penetration tests (in Portuguese). Federal University of Rio de Janeiro: M.Sc. Thesis.

Minato, K.K., Cantini, C.V. & Teixeira, M.G. 2009. Study and implementation of the Discrete Element Method. XXX Ibero-Latin-American Conference in Computational Methods in Engineering, Rio de Janeiro.

Munjiza, A. 2004 The Combined Finite-Discrete Element Method. London: John Wiley & Sons. ISBN 0-470-84199-0.

Oliveira, J.R.M.S. & Almeida, M.S.S. 2010. Pore-pressure generation in cyclic T-bar tests on clayey soil. International Journal of Physical Modelling in Geotechnics 10, No. 1, 19–24. DOI 10.1680/ijpmg.2010.10.1.19.

Oliveira, J.R.M.S., Almeida, M.S.S., Almeida, M.C.F. & Borges, R.G. 2010. Physical Modeling of Lateral Clay-Pipe Interaction. J. Geotech. Geoenviron. Eng. 136, No. 7, 950-956, DOI 10.1061/(ASCE)GT.1943-5606.0000311.

Oliveira, J.R.M.S., Almeida, M.S.S., Motta, H.P.G., & Almeida, M.C.F. 2011. Influence of Penetration Rate on Penetrometer Resistance. J. Geotech. Geoenviron. Eng. 137, No. 7, 695-703, DOI 10.1061/(ASCE)GT.1943-5606.0000480.

Randolph, M.F. & Houlsby, G.T. 1984. The limiting pressure on a circular pile loaded laterally in cohesive soil. Géotechnique 34, No. 4, 613–623.

Silva, V.M., Carvalho, L.S., Oliveira, J.R.M.S. & Marques, M.E.S. 2011 Virtual fall cone tests using Discrete Element Method. 14th Pan-American Conference on Soil Mechanics and Geotechnical Engineering, Toronto.

Stewart, D.P. & Randolph, M.F. 1991. A new site investigation tool for the centrifuge. Colorado: International Conference on Centrifuge Modeling. p. 531-538.

Stewart, D.P. & Randolph, M.F. 1994. T-Bar Penetration Testing in Soft Clay. Journal of Geotechnical Engineering 120, No. 12, p. 2230-2235.